様　式　Ｃ－１９、Ｆ－１９－１、Ｚ－１９　（共通）

科学研究費助成事業　　研究成果報告書

令和　６ 年　 ６ 月 １４ 日現在

機関番号：１４４０１
研究種目：若手研究
研究期間：2022～2023
課題番号：２２Ｋ１４５１０

研究課題名（和文）Oxide Accelerating Primary Ferrite Nucleation of Austenitic Stainless Steel Weldment

研究課題名（英文）Oxide Accelerating Primary Ferrite Nucleation of Austenitic Stainless Steel Weldment

研究代表者
HOU　YUYANG（HOU, YUYANG）

大阪大学・接合科学研究所・助教

研究者番号：６０９０５９３３

交付決定額（研究期間全体）：（直接経費）　　3,500,000円

研究成果の概要（和文）：FAモードで凝固されたステンレス鋼において、初晶フェライト核形成（PFN）は酸化物+TiNによって加速されました。PFNに効果的な酸化物はTi2O3、(Al,Ti)OxおよびMgAl2O4であり、このうちMgAl2O4が最適な酸化物です。PFNはδフェライトの形態をネットワークからランダムなバミキュラーδへと顕著に変化させました。しかし、オーステナイトの形態に対するPFNの影響は限定的であり、オーステナイトの形成と成長は初晶フェライトとは独立していました。引張り破壊が誘発される脆いTiNの形成により、引張り強度および延性が悪化しました。

研究成果の学術的意義や社会的意義
This research developed a new method for primary ferrite nucleation in stainless steel with FA mode. These results offer an effective method for the control of weld microstructure. The fracture mechanism offers an important guidance for further improvement of mechanical performance.

研究成果の概要（英文）：In this study, primary ferrite nucleation (PFN) was accelerated by Oxide+TiN to achieve the equiaxed δ-ferrite of stainless steel with FA solidification mode. The effective oxide for PFN was revealed as Ti2O3, (Al,Ti)Ox, and MgAl2O4, where MgAl2O4 is the optimal oxide. Under the double side bead on plate welding, the PFN was achieved by Ti-Al-Mg alloying, and significantly transformed the δ-ferrite form network morphology to random Vermicular-δ. However, PFN have limited influence on austenite formation under FA mode because the formation and growth of austenite were independent to the primary ferrite. The UTS and elongation was deteriorated by PFN, because the formation of fragment TiN initiated the tensile fracture.

研究分野：材料加工および組織制御関連

キーワード：Stainless steel　Weld metal　Nucleation　Grain refinement　Solidification　Tensile property

１．研究開始当初の背景

Austenitic stainless steels solidified with primary ferrite (FA mode austenitic stainless steel, FA–ASS) are widely used for excellent corrosion resistance and mechanical properties and the most extensive grade is SUS304. Lightweight and energy-saving put forward high requirements for strength and toughness by sound FA–ASS weld. While the typical solidification structure in Weld Metal (WM) of FA–ASS is usually columnar-dendritic ferrite, which significantly deteriorates the mechanical properties. The equiaxed and fine-grained microstructure is an ideal solution. However, there still lacks of applicable methods for practical applications.

Therefore, it is desired to perform grain refinement, especially equiaxed ferrite solidification, to achieve high strength and toughness simultaneously. Nucleation was considered as an important method with high economic and practical potential for equiaxed ferrite formation. TiN is a widely recognized nucleus for δ–ferrite nucleation and was successfully applied in the casting processes. However, spontaneous crystallization of TiN requires high supersaturation. The high cooling rate and temperature gradient of welding are unfavorable for TiN crystallization and δ–ferrite nucleation. Recently, comprehensive alloying of Mg, Al, and Ti can greatly accelerate equiaxed solidification. Because some specific oxides such as Al_2MgO_4, Ti–Al–oxide, Ti_2O_3 dispersedly formed in liquid accelerated TiN crystallization and then promoted the TiN nucleating δ–ferrite.

However, it is still necessary to determine the optimal oxide. Although previous studies of Inoue et al. and the applicant reported the feasibility of PFN in the casting of FA–ASS, the validity of oxide in welding and its effect on mechanical properties need further investigation. Moreover, there still exists an argument about the optimal oxide type for ferrite nucleation and the acceleration mechanism.

２．研究の目的

In this study, it was proposed to apply the oxide technology to accelerate the primary ferrite nucleation (PFN) and equiaxed solidification of FA–ASS weldment, to obtain highly anisotropic and refined microstructure and achieve simultaneously improved strength and toughness. The effective oxide for primary ferrite nucleation, structure evolution mechanism, and mechanical property will be fully investigated and evaluated. The optimized compositional design will be proposed. The solidification and strengthening mechanism will be evaluated by experimental identification and theoretical calculation. This research will propose new strategies and knowledge in grain refinement, strengthening, and toughening.

３．研究の方法

In this study, four major contents were conducted, (1) finding out the optimal oxide for PFN using Fe–16Cr stainless steel to avoid the influence of phase transformation; (2) exploring the composition of FA mode solidification with PFN accelerated by optimal oxide to prevent the shift of solidification mode after alloying; (3) investigating the weld microstructure evolution and elucidating the nucleation mechanism; (4) evaluating the mechanical properties of FA–ASS weld and revealing the failure mechanism.

Commercial Type 304 and 430 stainless steel was used as the base metal. The additional materials include sponge titanium, aluminum block, and Ni-50% Mg alloy. The base metal and additions were melted to fabricate master alloy using a gas tungsten arc (GTA) button-melting device with 200A for 1 min. The button specimens were then cut into block specimens of 25 mm length, 5 mm height, and 6 mm width. The block specimens with modified elemental compositions were welded to base metal plates using double-sided bead-on-plate GTA welding. In the welding process, the current was 150 A, the welding speed was 100 mm/min, and the arc length was 3 mm as shown in Fig. 1.

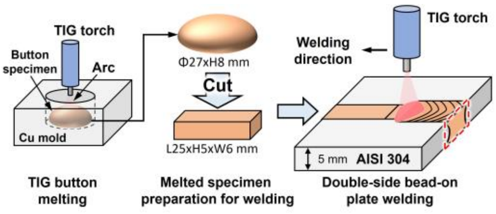

Fig. 1 Experimental procedure in this study.

The compositions of the weld metals were analyzed by inductively coupled plasma atomic emission spectroscopy (ICP-AES, ICPV-1017, SHIMADZU) as well as C/S, and O/N analyzers. The weld metals of the GTA button and welded specimens were cut and polished in the cross-sectional direction. The microstructures were observed using optical microscopy (OM, VHX-7000, KEYENCE) and scanning electron microscopy (SEM, SU1510, HITACHI) with electron backscatter diffraction (EBSD; EDAX DigiView, AMETEK). The composition of the microconstituents was investigated using energy-dispersive X-ray spectroscopy (EDS; EDAX Elect Plus, AMETEK) on SEM. The phase morphology and orientation relationship (OR) were investigated by analyzing the EBSD data to identify the primary ferrite nucleation and austenite formation.

The tensile test focused on the weld metal of the as-welded specimens. The tensile direction was perpendicular to the welding direction along the dimensions of the tensile specimens. The gauge length was 4 mm, and Vickers points (0.5 mm) were marked for direct strain measurements using a high-speed camera.

The crosshead speed during the tensile test was set to 1 mm/min. After the tensile test, the surface and cross-section of the fracture were investigated by SEM and EDS to determine the failure morphology.

４．研究成果

(1) Exploration of the optimal oxide for primary ferrite nucleation.

Fig. 2 reveals the microstructure, alloying condition, and microconstituent. Non-added and TiN are composed of columnar grains, where the TiN specimen was alloyed with Ti and excessive Al to decrease the [O] as much as possible. The grain of non-added is coarser than that of TiN specimen. In Ti, Al-Ti, and Mg-Al-Ti specimens, the microstructures all exhibit a high area ratio of equiaxed grain, with the highest in the Mg-Al-Ti specimen. The microconstituents transferred from (Si, Cr)Ox in non-added to TiN in TiN specimen and Oxide+TiN in Ti, Ti-Al, and Ti-Al-Mg specimens.

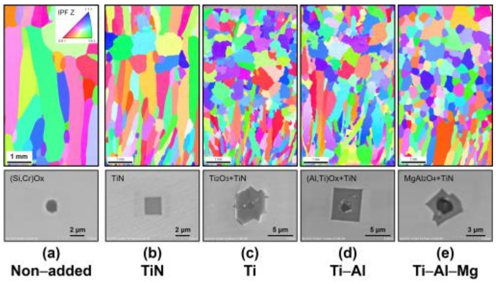

Fig. 2 Microstructure and microconstituents varied with alloying conditions.

The number and average equivalent circular diameter (ECD) of microconstituents were investigated within 6.45 mm^2 of each specimen. The number of TiN in TiN specimen was above 600 counts and became low as about 300 ~ 450 counts in Ti, Al-Ti, and Mg-Al-Ti specimens. The number of Oxide+TiN increased in Ti, Al-Ti, and Mg-Al-Ti specimens as compared with TiN specimen. The ECD of TiN is about 2 μm as same as the (Si, Cr)Ox, while Oxide+TiN is in the range of 3 ~ 5μm. The number ratio of Oxide+TiN to total microconstituents is positively related to the area ratio of equiaxed grain. Oxide+TiN was considered as the effective inoculant for δ-ferrite nucleation. The TiN formation of Oxide+TiN was accelerated by oxide. The accelerating effect in the Mg-Al-Ti alloying specimen is the most obvious.

(2) Exploration of the composition in FA mode solidification with PFN.

The addition of Ti, Al, and Mg promotes the transformation from FA to F mode during solidification. The microstructure and orientation with different Ni_{eq} were revealed as shown in Fig. 3 using the inverse pole figure (IPF) map. The microstructures at ambient temperature are mainly composed of the γ phase. The γ grain of the Non-added specimen shows columnar morphology. In the specimens from #1 to #3, the columnar γ grain still developed with a small area of equiaxed γ grain appearing in the top part. In specimen #4, simi-equiaxed γ grain was promoted, and fine equiaxed γ grain appeared in specimen #5.

$MgAl_2O_4$+TiN was observed in all the alloyed specimens from #1 to #5, acting as nuclei to nucleate the equiaxed δ for the equiaxed primary ferrite grain. However, the γ morphology did not show a significant difference in FA mode, which could be attributed to the independent growth between δ and γ. Therefore, the γ grain still grew as columnar in the specimens from #1 to #4 due to FA mode. In summary, the fine equiaxed ferrite grain could be formed by $MgAl_2O_4$+TiN as the primary phase in austenitic stainless steel. However, accelerating the formation of fine equiaxed austenite grains requires both the PFN and austenite formation during FA mode solidification.

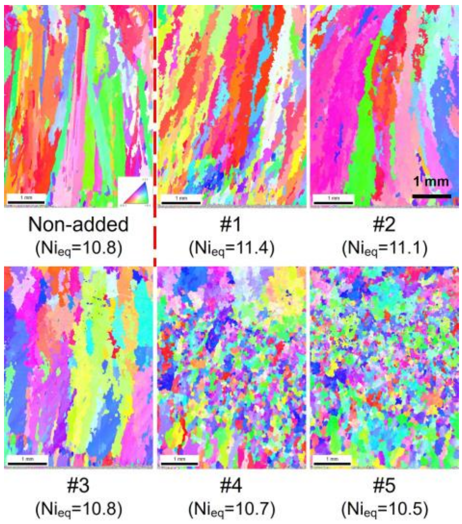

Fig. 3 As-solidified structure.

(3) Investigation of the weld microstructure and evolution mechanism.

The optimal conditions for PFN and FA solidification mode were applied in the double-side bead on plate welding. The microstructure and evolution mechanism of the weld metal of FA-ASS is shown in Fig. 4.

The microstructures show the orientation of austenite and ferrite, where austenite occupied the majority due to the small amount of ferrite. It indicates that no significant difference was achieved in the FA mode with or without alloying of Ti, Al, and Mg, which corresponded to the result in button melting conditions. In other words, the microstructures of both the Non-added (FA-Non) and Ti-Al-Mg (FA-TAM) specimens consisted predominantly of coarse columnar grains.

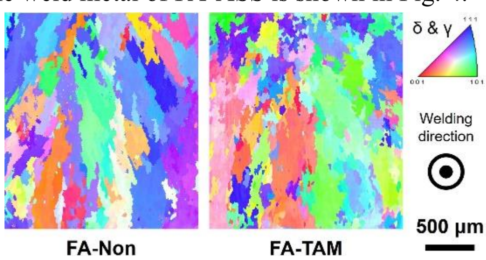

Fig. 4 As-welded microstructure.

Detailed observations were revealed in Fig. 5. The FA-Non specimen showed a network morphology of the residual ferrites, characterized by two distinct types of Vermicular-δ and Lacy-δ. A unique microstructure was observed in the FA-TAM sample where the network changed into random Vermicular-δ in the FA-TAM specimen, indicating the alloying of Ti, Al, and Mg could nucleate the primary ferrite. The PFN accelerated by Ti-Al-Mg alloying can significantly refine the ferrite while having limited influence on austenite formation under FA mode. Therefore, detailed microstructural evolution was further investigated.

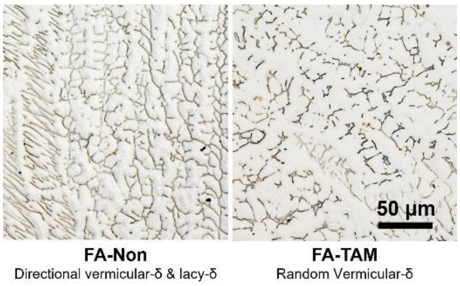

Fig. 5 The ferrite morphology in weld metal.

The crystallographic ORs of the FA-TAM specimens were obtained from the EBSD results, as shown in Fig. 6. $MgAl_2O_4$, TiN, ferrite, and austenite were identified in FA-TAM specimens. Notably, $MgAl_2O_4$ was located at the center of TiN, and TiN was directly connected to the ferrite. The ferrite consistently solidified as the primary phase. The primary ferrite was subsequently transformed into an austenite phase in the solid state after solidification. The direct contact of TiN to the primary ferrite indicates that TiN may nucleate the primary ferrite.

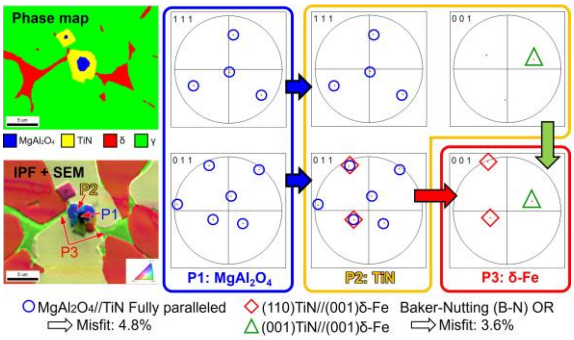

Fig. 6 Orientation relationships and misfit.

The crystallographic orientations of $MgAl_2O_4$ and TiN were fully parallel, as indicated by the blue circles. Such OR indicates the lattice misfit between them is considered as 4.8%, suggesting that $MgAl_2O_4$ can accelerate the formation of TiN. The ORs between TiN and ferrite were identified as 001TiN//001Fe and 011TiN//001Fe, as indicated by green triangles and red rhombuses, respectively. This specific OR is known as the Baker–Nutting (B–N) OR. Under these orientation conditions, the lattice misfit between TiN and ferrite is determined as 3.6%. These results imply that TiN promotes ferrite nucleation. Therefore, $MgAl_2O_4$ accelerated the formation of TiN and promoted the primary ferrite nucleation.

The effects of the alloying and solidification modes on the microstructure were illustrated. The alloying of Ti, Al, and Mg consistently facilitated the nucleation of primary ferrite, leading to the formation of refined equiaxed ferrite. Austenite originates in the residual liquid phase through a eutectic reaction during solidification and grows epitaxially toward ferrite from the base metal after solidification. The formation and growth of austenite were independent of the primary ferrite. The morphology and orientation of the ferrite could hardly influence the formation and growth of austenite. Therefore, the austenite continues to form as columnar.

(4) Mechanical properties and failure mechanism of FA–ASS weld with PFN.

The stress-strain curves of the specimens are shown in Fig. 7. The red line signifies the FA-Non specimen, whereas the blue line represents the FA-TAM specimen. A summary of the UTS and elongation indicates that the addition of Ti, Al, and Mg deteriorated the tensile properties of the FA-TAM specimens.

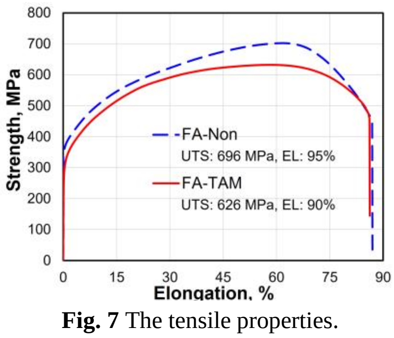

Fig. 7 The tensile properties.

The morphologies of the tensile fracture surfaces and in the cross-section of the specimens revealed ductile dimples as shown in Fig. 8. However, TiN was observed at the center of the dimples after alloying of Ti, Al, and Mg to the specimens. Further observation in the fracture cross-sections indicates that fragment TiN was observed at the root of the dimples, which is consistent with the observation of the fracture surface. Given the inherent brittleness of TiN, this fragmentation is likely attributable to its low ability to resist material deformation during the tensile test. Consequently, TiN can be considered to initiate fracture to degrade tensile properties.

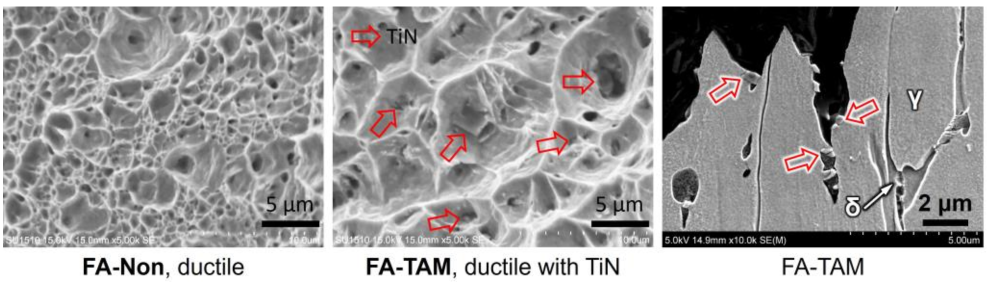

Fig. 8 The fracture morphology

５．主な発表論文等

〔雑誌論文〕　計2件（うち査読付論文　2件／うち国際共著　1件／うちオープンアクセス　0件）

１．著者名 Hou Yuyang、Kadoi Kota	４．巻 204
２．論文標題 Nucleation of equiaxed δ-ferrite by accelerating TiN formation controlled by oxide during welding of ferritic stainless steel	５．発行年 2023年
３．雑誌名 Materials Characterization	６．最初と最後の頁 113212～113212
掲載論文のDOI（デジタルオブジェクト識別子） 10.1016/j.matchar.2023.113212	査読の有無 有
オープンアクセス オープンアクセスではない、又はオープンアクセスが困難	国際共著 －

１．著者名 Hou Yuyang、Cheng Guoguang、Kadoi Kota、Inoue Hiroshige	４．巻 912
２．論文標題 Acceleration mechanism of Ti2O3 on TiN formation and δ-ferrite nucleation of ferritic stainless steel	５．発行年 2022年
３．雑誌名 Journal of Alloys and Compounds	６．最初と最後の頁 165221～165221
掲載論文のDOI（デジタルオブジェクト識別子） 10.1016/j.jallcom.2022.165221	査読の有無 有
オープンアクセス オープンアクセスではない、又はオープンアクセスが困難	国際共著 該当する

〔学会発表〕　計3件（うち招待講演　0件／うち国際学会　0件）

１．発表者名 侯 雨陽、門井 浩太
２．発表標題 FA と F モード凝固するオーステナイト系ステンレス鋼溶接金属の引張特性に及ぼすフェライト結晶粒微細化の影響
３．学会等名 （一社）溶接学会 2023年度秋季全国大会
４．発表年 2023年

１．発表者名 侯 雨陽、門井 浩太
２．発表標題 フェライト系ステンレス鋼溶接金属でのδフェライト核生成促進のためのTiN生成に及ぼす酸化物の影響
３．学会等名 （一社）溶接学会 2022年度 秋季全国大会
４．発表年 2022年

１．発表者名 侯 雨陽、門井 浩太
２．発表標題 FAモード凝固における オーステナイト形成に及ぼす フェライト結晶粒微細化の影響
３．学会等名 （一社）溶接学会 2023年度 春季全国大会
４．発表年 2023年

〔図書〕　計0件

〔産業財産権〕

〔その他〕

－

６．研究組織

	氏名 （ローマ字氏名） （研究者番号）	所属研究機関・部局・職 （機関番号）	備考

７．科研費を使用して開催した国際研究集会

〔国際研究集会〕　計0件

８．本研究に関連して実施した国際共同研究の実施状況

共同研究相手国	相手方研究機関